Thin Solid Films 517 (2009) 5172–5175

Contents lists available at ScienceDirect

Thin Solid Films

journal homepage: www.elsevier.com/locate/tsf

Novel structural functional films based on self-assembly template and electrodeposition: Synthesis and characterization of porous Ni/YSZ films

Bin Ma [a], Yao Li [a,*], Jiupeng Zhao [b], Xue Li [b], Wuhong Xin [b]

[a] Center for Composite Materials, Harbin Institute of Technology, No. 2 Yikuang Street, Nangang District, Harbin 150080, PR China
[b] School of Chemical Engineering and Technology, Harbin Institute of Technology, No. 92 Xidazhi Street, Nangang District, Harbin 150001, PR China

ARTICLE INFO

Available online 20 March 2009

Keywords:
Self-assembly PS template
3DOM nickel films
YSZ film

ABSTRACT

Three-dimensionally ordered macroporous (3DOM) nickel films are fabricated by electro-deposition into the interstitial spaces of polystyrene (PS) template formed by PS latex spheres self-assembled on nickel alloy substrates. Yttria stabilized zirconia (YSZ) precursor prepared by the sol–gel method is infiltrated in the voids of the 3DOM nickel films. After heat treatment, a novel structure of 3DOM nickel films with YSZ filled in the hollow regions (3DOM Ni/YSZ composite) has been obtained. Structure and surface morphology of the specimens were studied by X-ray diffractometry (XRD) and scanning electronic microscopy (SEM), respectively. The thermal analysis (TG-DTA) was carried out to study the thermal decomposition process of YSZ gel. When the compound specimen is calcined at 600 °C or higher temperature, the YSZ with cubic structure phase can be prepared.

© 2009 Elsevier B.V. All rights reserved.

1. Introduction

Much attention has been focused on three-dimensionally ordered macroporous (3DOM) materials in recent years, because of their unique properties and potential applications in photonic crystals, catalysis, sensors, hierarchic battery electrodes etc. [1–6]. As we know, porous nickel materials with high surface area and nanoarchitectures as well as important physical properties, have been of great interest owing to its broad applications in the fields of catalysts, high-density data storage, lightweight structure, electrodes, and sensors [7–14]. Furthermore, the nickel alloy can retain its excellent properties in the high temperature. To our knowledge, ITO glass, alumina, Au, and silicon substrates are usually used in fundamental researches [15–18]. No reports about using the nickel alloy as the substrate are found.

Yttria stabilized zirconia (YSZ) film or coating is becoming increasingly important because of a variety of applications such as sensors, catalysts, electrodes, buffer layers, separation media and thermal insulators [19–22]. But due to the change of temperature and shape of the devices, the YSZ film or coating will strip away from the substrate. To avoid the failure of films or coatings in the high temperature and to fabricate the multifunctional films, we fabricate the 3DOM nickel films on the nickel alloy substrate and the YSZ film in the porous Ni films. The interface between YSZ and Ni framework become much larger which effectively increases the reaction area. We hope the structure of 3DOM Ni/YSZ composite can give an inspiration to those who are researching solid oxide fuel cell (SOFC), catalysts, electrodes and sensors.

In this paper, the electro-deposition through self-assembly templates has been used for the preparation of 3DOM nickel films. The templates were prepared by self-assembly of polystyrene latex spheres on a nickel alloy substrate. YSZ film was prepared by the sol–gel method based on the 3DOM nickel films.

2. Experimental details

The preparation process of the 3DOM nickel films is illustrated in Fig. 1. Monodisperse polystyrene spheres latex with an average diameter of 500 nm were obtained by using an emulsifier free emulsion polymerization technique [23]. The templates were prepared by self-assembly of polystyrene latex spheres on a nickel alloy substrate which was polished and cleaned. The chemical composition of the substrate is shown in Table 1. The substrate was put into 1 wt.% polystyrene spheres latex. Subsequently, the water was allowed to evaporate slowly for 2–3 days. During evaporation the PS spheres self-assembled by capillary and electrostatic forces into 3D close packed structure. This ordered structure of spheres forms the ordered PS templates. Then the nickel alloy substrates with the ordered PS template were immersed into the electrolyte at 40 °C, and the interstice networks of the templates were filled with nickel deposits at a constant cathode current density of 0.3 Acm^{-2}. By electro-deposition, the porous nickel films were finally obtained by dissolving the PS templates in toluene for 2 days. The composition of the electrolyte and the deposition conditions are given in Table 2.

For the preparation of YSZ precursor, zirconium oxychloride and yttrium nitrate were dissolved in citric acid aqueous solution with the molar ratio of citric acid: $ZrOCl_2.8H_2O$: $Y(NO_3).6H_2O$ = 108: 92: 16. The solution was then evaporated at 80 °C to obtain a viscous YSZ

* Corresponding author. Tel./fax: +86 451 86402345.
E-mail address: liyao@hit.edu.cn (Y. Li).

0040-6090/$ – see front matter © 2009 Elsevier B.V. All rights reserved.
doi:10.1016/j.tsf.2009.03.076

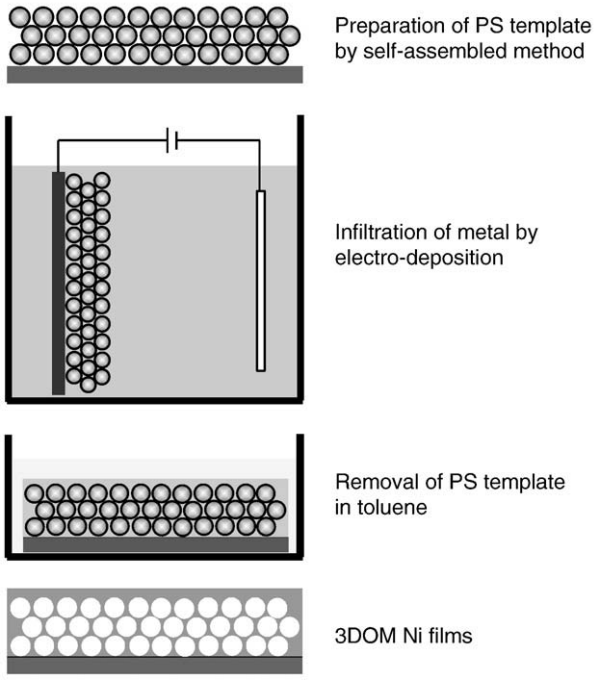

Fig. 1. Schematic diagrams of the preparation of macroporous nickel films.

precursor, which can be used to infiltrate into the voids of 3DOM nickel films. The obtained 3DOM nickel film/YSZ precursor composites were subsequently dried in the constant temperature furnace at 40 °C and then heated in air up to 700 °C for 2 h at a heating rate of 2 °C/min to obtain porous structure of 3DOM Ni/YSZ composite.

Structure and surface morphology of the specimens were studied by XRD and SEM, respectively. The XRD measurements were performed on a Rigaku D/max-rB X-ray diffractometer with Cu Kα radiation of 1.5418 Å. Morphological investigation was performed using a Philips MX2600 FEI scanning electron microscope. TGA was performed with a ZRY-2P thermogravimetric analyzer.

3. Results and discussion

The SEM images of PS template by self-assembly method are shown in Fig. 2. The synthesized PS template in this study displayed a hexagonal array as shown in Fig. 2, which indicated the most stable state of thermodynamics, although there were some point defects, line defects, and stacking defects in local places (Fig. 2a). There was some dislocation between the first layer and inner layer through the point defect which was considered to be a typical characteristic of the face-centred cubic (fcc) packing structure. In small regions, the perfect PS templates were obtained as shown in the Fig. 2b.

Since the macroporous structure of the materials synthesized using this technique is the inverse of the original template, the regularity of the packing of the voids directly reflects the quality of the packing of the spheres in the original template (Fig. 2). Fig. 3a shows a large scale SEM image for a macroporous nickel film which possesses an ordered porous structure with uniform spherical pores. The micrograph shows that the array of pores embedded in

Table 1
Chemical composition of Ni alloy substrate.

Elements	Ni	Cr	Al	Fe	Mn	Si	Zr	C	B	Y
Content (wt.%)	75	16	4.5	3	0.5	0.2	0.1	0.05	0.01	0.01

Table 2
Composition of electrolyte and conditions used in the electro-deposition of Ni films.

	Ni plating solution
$NiSO_4 \cdot 6H_2O$	300 gL^{-1}
$NiCl_2 \cdot 6H_2O$	45 gL^{-1}
Boric acid	30 gL^{-1}
Sodium dodecyl sulfate(SDS)	0.05 gL^{-1}
pH (adjusted by H_2SO_4)	3.5–4
Cathode current density	0.3 $mAcm^{-2}$
Deposition potential	10 V

the nickel matrix are arranged in a multidomain (polycrystalline) structure with the domain size about 100 um^2. Fig. 3a also shows the presence of pore crystal lattice defects (shown by the arrows) such as terrace dislocations and point defects. Defects of this type are commonly observed due to defects in the packing of the original template. The SEM images reveal a face-centered cubic structure of spherical pores in the nickel framework (Fig. 3b), which is consistent with the PS templates structure. The average center-to-center distance between close-packed voids is 500 nm, suggesting no structure shrinkage during the fabrication process. The addition of sodium dodecyl sulfate (SDS) surfactant to the eletrolyte has the desired effect of significantly reducing the sub-micron roughness of the macroporous nickel film so that it can replicate the template structure better with a more uniform thickness [8].

In order to determine the crystal structure of the porous nickel film and to estimate the crystal grain size we have carried out X-ray diffraction measurements on the nickel films. Fig. 4a shows X-ray

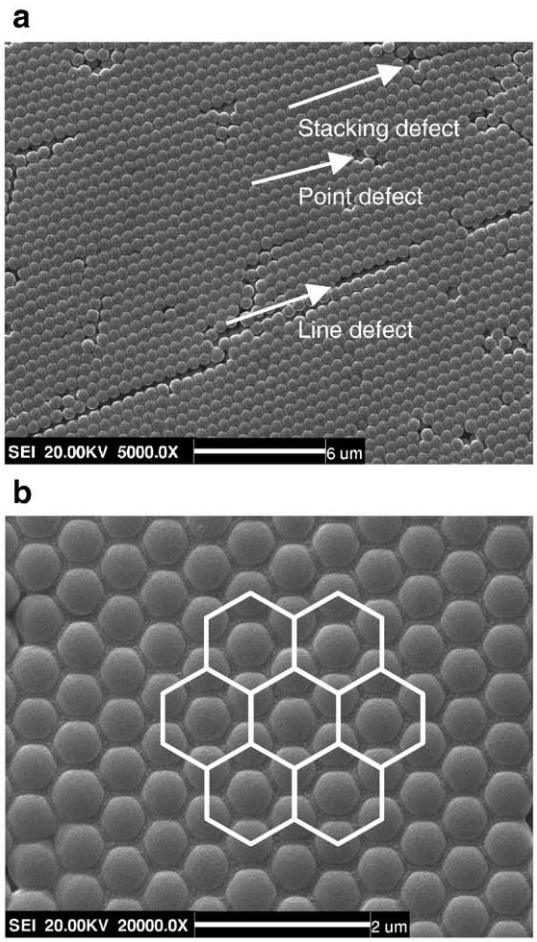

Fig. 2. SEM images of the PS template with (a) low magnification and (b) high magnification.

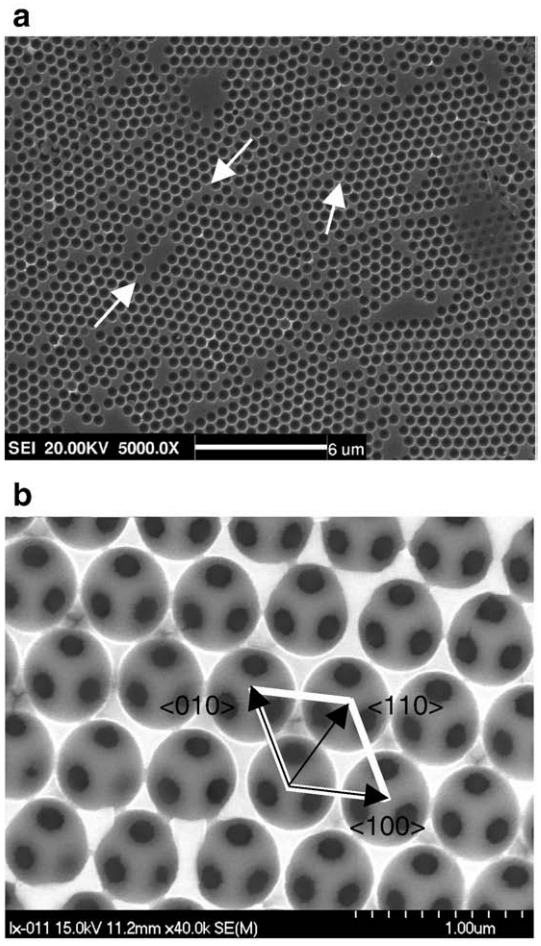

Fig. 3. Low (a) and high (b) magnification SEM images of macroporous nickel films.

diffraction patterns of ordered macroporous nickel structures. The diffraction patterns show (111), (220), (311), and (222) peaks. The X-ray diffraction pattern clearly shows the characteristic reflections for a highly polycrystalline film with a face-centred cubic (fcc) crystal structure. As shown, the elements contained in the substrate (Table 1) are not detected in this pattern of Fig. 4 except Ni. So the peaks reported in the Fig. 4 originate in the Ni deposited porous structure, but not from the Ni alloy substrate. The crystal structure of the film is consistent with the results obtained for the non-templated (nonporous) films [8,16]. The mean gain sizes of the film are evaluated by using the Debye-Scherer formula [24]:

$$D = \frac{K\lambda}{W \cdot \cos\theta}$$

where K is usually nearly 1, λ is the X-ray wavelength (1.5418 Å), θ is the Bragg diffraction angle, and W is the FWHM (full widths at half-maximum). The average grain size of the nickel films is 37.8 nm. A similar crystalline grain size was obtained for normal (non-templated) electrodeposited nickel films suggesting that the electrodeposition of the nickel within the interstitial spaces of the template does not alter the crystalline grain size of the deposited film [25]. Then the nickel film treated at 600 °C for 2 h is investigated by XRD. The result is shown in the Fig. 4b. Only a small part of nickel film (3%) is oxidated to form nickelous oxide (space group: Fm3 m (225)).

X-ray diffraction (XRD) analysis in the Fig. 5 indicates that the precursor is amorphous when heat-treated at 400 °C (Fig. 5a). With the increase in temperature up to 500 °C, the peaks intensify sharply. While treated at 500 °C for 2 h, partial crystallization of YSZ appears, since the intensities of some primary peaks enhance and additional diffraction peaks occur. As shown in Fig. 5c, when the precursor is treated at 600 °C for 2 h the cubic phase of YSZ is formed as we have expected. Higher temperature such as 700 °C in the Fig. 5d has the advantages of crystallization of the desired phase. In order to prevent

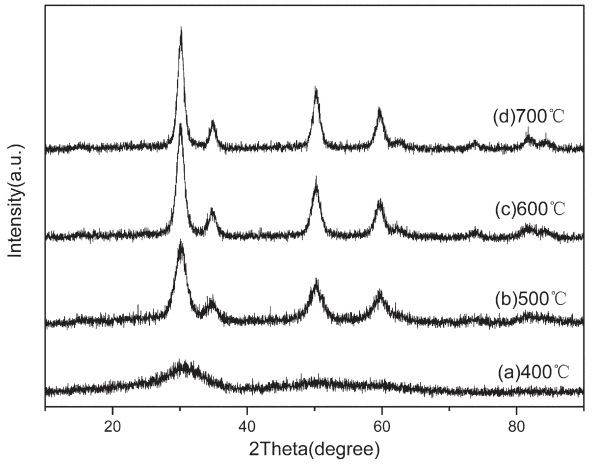

Fig. 5. XRD pattern of porous YSZ calcined at (a) 400 °C,(b) 500 °C, (c) 600 °C and (d) 700 °C for 2h in ambient air.

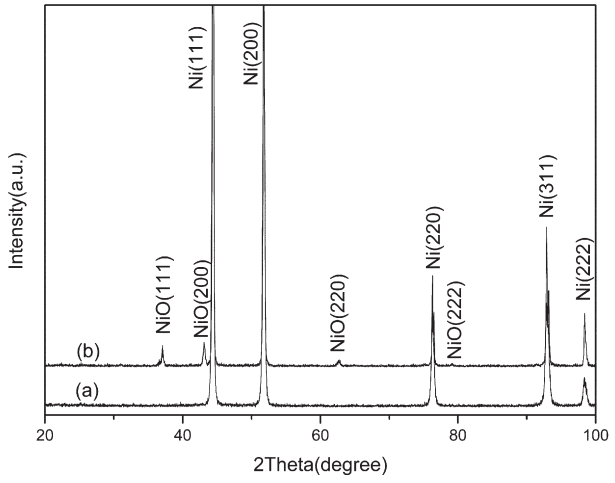

Fig. 4. XRD pattern of (a) the 3DOM nickel films and (b) the films treated at 600 °C for 2h.

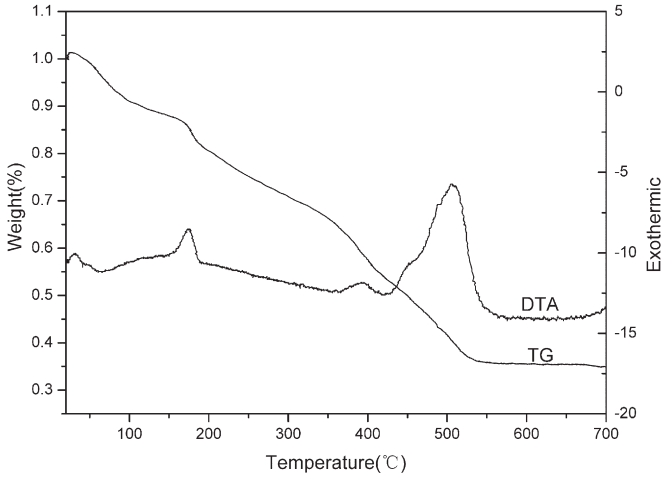

Fig. 6. TG-DTA curves of the YSZ gel.

the substrate from high temperature deformation, we thus choose 600 °C as the final sintering temperature.

TG-DTA curves of the YSZ gel was shown in Fig. 6. The first weight loss of 9.12% occurred between 41 °C and 100 °C which was accompanied by an endothermal peak due to the loss of physically adsorbed water. The decomposition of the citric acid and the loss of physically adsorbed water further led the weight loss about 38.22% between 100 °C and 429 °C, and a strong exothermic peak of citric acid appeared at 173.1 °C. The weight loss of 15.7% was observed between 429 °C and 525.8 °C, which was attributed to the decomposition of organic species. From 525.8 °C to 700 °C, the weight remained constant approximately indicating the organic species decomposed completely. The TG–DTA results were consistent with the XRD pattern showed in the Fig. 5.

4. Conclusions

In summary, the PS templates were prepared by self-assembly of polystyrene latex spheres on a nickel alloy substrate, which is displayed a hexagonal array. 3DOM nickel films on the nickel alloy substrate could be obtained by using the electro-deposition through the PS templates, which possesses a face-centred cubic (fcc) crystal structure. The average nickel grain size of the nickel film is 37.8 nm. The precursor of YSZ was used to infiltrate into the voids of 3DOM nickel film. The cubic phase of YSZ was formed when the precursor of YSZ was treated at 600 °C for 2 h. Like the steel skeletons in the reinforced concrete, the 3DOM nickel films on the nickel alloy substrate are the skeletons in the YSZ film to strengthen the combination between YSZ film and the nickel alloy substrate.

Acknowledgements

We thank the National Natural Science Foundation of China (No.20601006), Program for New Century Excellent Talents in University (NCET-06-0335), Natural Scientific Research Innovation Foundation in HIT (200804) and CAST Foundation for financial support.

References

[1] J.I.L. Chen, G. Freymann, S.Y. Choi, V. Kitaev, G.A. Ozin, Adv. Mater. 18 (2006) 1915.
[2] R.C. Schroden, M. Al-Daous, S. Sokolov, B.J. Melde, J. Mater. Chem. 12 (2002) 3261.
[3] B.J.S. Johnson, A. Stein, Inorg. Chem. 40 (2001) 801.
[4] C. López, Adv. Mater. 15 (2003) 1679.
[5] T. Cassagneau, F. Caruso, Adv. Mater. 14 (2002) 1837.
[6] W.P. Qian, Z.Z. Gu, A. Fujishima, Langmuir 18 (2002) 4526.
[7] R. Han, W. Pan, Mater. Lett. 61 (2007) 5014.
[8] P.N. Bartlett, M.A. Ghanem, J. Mater. Chem. 13 (2003) 2596.
[9] G. Duan, W. Cai, J. Phys. Chem. B 110 (2006) 7184.
[10] A. Goncharov, A.A. Zhukov, J. Magn. Magn. Mater. 286 (2005) 1.
[11] A.A. Zhukov, A. Goncharov, J. Appl. Phys. 93 (2003) 7322.
[12] O.D. Velev, P.M. Tessier, A.M. Lenhoff, E.W. Kaler, Nature 401 (1999) 548.
[13] K.M. Kulinowski, P. Jiang, H. Vaswani, V.L. Colvin, Adv. Mater. 12 (2000) 833.
[14] O.D. Velev, E.W. Kaler, Adv. Mater. 12 (2000) 531.
[15] A. Matsuda, S. Akiba, Thin Solid Films 516 (2008) 3873.
[16] Y. Tang, D. Zhao, Thin Solid Films 516 (2008) 2094.
[17] J.T. Abiade, G.X. Miao, Thin Solid Films 516 (2008) 2082.
[18] Y.W. Hao, F.Q. Zhu, C.L. Chien, J. Electrochem. Soc. 154 (2007) D65.
[19] C. Cantoni, D.K. Christen, R. Feenstra, Appl. Phys. Lett. 79 (2001) 3017.
[20] S.P. Jiang, S.H. Chan, J. Mater. Sci. 39 (2004) 4405.
[21] K.W. Schilichting, N.P. Padture, P.G. Kelemens, J. Mater. Sci. 36 (2001) 3003.
[22] C. Viazzi, J.P. Bonino, F. Ansart, Surf. Coat. Technol. 201 (2006) 3889.
[23] J.H. Kim, M. Chainey, J. Polym. Sci., A, Polym. Chem. 27 (1989) 3187.
[24] B.D. Cullity, Elements of X-ray Diffractions, Addition-Wesley, Reading, MA, 1978, p. 102.
[25] S. Meguro, T. Sasaki, J. Electrochem. Soc. 147 (2000) 3003.